Effect of heating mode on sinterability of carbonyl iron compacts

A. Raja Annamalai*[1], F. Nekatibeb[1], A. Upadhyaya[1] and D. K. Agrawal[2]

In recent years, microwave processing has gained wide acceptance as a novel method for sintering metal powders. As compared to conventional sintering, microwave sintering provides rapid and volumetric heating involving conversion of electromagnetic energy into thermal energy within the material. This results in finer microstructures, thereby providing improved mechanical properties and quality of the products. This study examines the dependence of densification, microstructure and mechanical properties on the heating mode of Fe–2%Cu and Fe–2%Cu–0·8%C. The powdered compacts were sintered in conventional (radiation mode) and microwave (2·45 GHz, multimode) furnaces at 1120°C in $90N_2$–$10H_2$ atmosphere, and comparative analysis of the properties was investigated.

Keywords: Conventional sintering, Microwave sintering, Iron copper, Copper steel, Mechanical properties

Introduction

In ferrous powder metallurgy, it is a common practice to add copper and graphite as alloying elements to improve the mechanical properties of iron. Iron–copper steels (FC-02XX) are the most widely used structural powder metallurgy materials. Copper is added in elemental form. During sintering, copper melts at 1083°C and facilitates the formation of interparticle bonds between iron particles. In addition, the melt distributes itself in the network of pores in the compact, and from there, it diffuses into iron powders to form a solid solution, leaving large pores (secondary pores) behind. At high temperature (1250°C), the maximum amount of copper that can dissolve in austenite is from 8 to 10 wt-%, but upon cooling, the excess amount of copper in the supersaturated solid solution precipitates out, which in turn strengthens the material (precipitation hardening). Copper contents above 2% show copper precipitates in either the grain boundaries or at prior particle boundaries. Apart from the improvement in mechanical properties, copper addition also causes swelling during sintering, which is termed as copper growth. This effect has been extensively investigated by various researchers.[1–8] In a similar manner, carbon is added to increase strength and hardness by forming a pearlite microstructure. Added to the benefits in mechanical properties, carbon has been used as a means of reducing the swelling induced by copper melt penetration.[5,7] Some of the most common alloy systems in ferrous powder metallurgy are iron–copper (Fe–2–Cu) and copper steel (Fe–2Cu–0·8C). These alloys have been widely used for automotive applications due to their lower cost of production and near net shaping, which satisfies close dimensional tolerance requirements for parts with complex geometries and reduces the need for secondary machining. In order to meet the requirements of more demanding applications, with regard to improved mechanical properties and lower production cost, in recent years, there has been a trend towards a microwave processing technique for sintering these alloys systems. Roy *et al.*[9,10] showed, for the first time, an effective sinterability of iron, iron copper (Fe–Cu) and copper steel composition Fe–2Cu–0·8C in microwave. They have made comparative evaluation of green density, sintered density, hardness and modulus of rupture for the iron–copper (Fe–Cu) alloy system. Though the sintering conditions were not specifically mentioned for iron–copper (Fe–Cu), they found out that the microwave sintered samples exhibited better density, hardness and modulus of rupture. Anklekar *et al.*[11–13] have reported microwave sintering of powder metallurgy (PM) copper steel (Fe–2Cu–0·8C) and comparative evaluation of mechanical properties using both microwave and conventional sintering techniques. They have reported that the microwave sintered samples exhibited finer microstructure, higher densification, hardness and flexural strength as compared to the conventionally sintered samples. However, to date, as per the author's knowledge, no investigation has been performed on the densification and mechanical properties of microwave sintered carbonyl iron and Fe–2Cu. In addition, there was no comparison of microwave sintered copper (Fe–2Cu–0·8Gr) steel with microwave sintered iron and iron copper (Fe–2Cu) before. This present study examines the sintering response of carbonyl Fe, Fe–2Cu and Fe–2Cu–0·8C alloys that have been consolidated through conventional and microwaves routes, and its compares the densification, microstructural evolutions and mechanical properties.

[1]Department of Materials Science and Engineering, Indian Institute of Technology Kanpur, Uttar Pradesh 208016, India
[2]Materials Research Institute, The Pennsylvania State University, University Park, PA 16802, USA

*Corresponding author, email araja@iitk.ac.in

Received 29 August 2011; accepted 11 February 2012
DOI 10.1179/1433075X12Y.0000000011

Experimental

For the present investigation, carbonyl iron powder (Sigma-Aldrich, USA), copper powder (Metal Powder Company Ltd, India) and graphite powder (K5, 15) (Lonza Ltd, Switzerland) were used as starting materials. The as received powders were characterised for particle morphology (size and shape) and flow behaviour as per the Metal Powder Industries Federation standard,[14–16] and the data are shown in Table 1. The morphology of the powders was obtained by a scanning electron microscope (Zeiss Evo 50, Carl Zeiss SMT Ltd, UK), and it is shown in Fig. 1. The powders were mixed in the required proportions (Fe–2Cu and Fe–2Cu–0·8Gr) in a turbula mixer (model T2C, Bachoffen, Switzerland) for 60 min. The mixed powders were pressed at 600 MPa to make cylindrical pellets (height ~6 mm, and diameter ~16 mm) using a uniaxial semiautomatic hydraulic press (model CTM-100, Blue star, India) using zinc stearate as die wall lubricant. The green compacts (as pressed) were sintered through conventional and microwave modes. Conventional sintering of the cylindrical pellets and other specimens was carried out in a $MoSi_2$ furnace at a constant heating rate of 5°C min^{-1} in a tubular furnace (OKAY 70T7, Bysakh & Co, India). A 15 min intermediate hold was given at 540 and 840°C to ensure uniform distribution of temperature during heating, intermittent and isothermal soaking. Microwave sintering of the green compacts was carried out using a multimode cavity 2·45 GHz, 6 kW commercial microwave furnace (Cober Electronics, CT, USA). The samples were sintered at 1120°C for 1 h in forming gas 95%N_2 and 5%H_2. The temperature of the sample was monitored using an infrared pyrometer (Raytek, Marathon Series) with the circular cross-wire focused on the sample cross-section The pyrometer is emissivity based; direct temperature measurement was measured above 700°C[17,18] by considering the emissivity of steel as (0·35).[19] Typically, emissivity varies with temperature. However, as very little variation in emissivity was reported in the temperature range used in the present study, hence, the effect of variation in emissivity was ignored. Further details of the experimental set-up of microwave sintering are described elsewhere.[20] The sintered density was obtained by dimensional measurements technique. The sintered density normalised with respect to the theoretical density based on the weight fraction (w) of the respective component. The theoretical density for a given composition (ρ_{th}) was calculated using the inverse rule of mixture and is expressed as

$$\frac{1}{\rho_T} = \sum_{i=1}^{N} \frac{w_i}{\rho_i} \tag{1}$$

Table 1 Powder characteristics of Fe, Cu and graphite powders

Characteristics		Fe	Cu	Graphite
Apparent density/g cm^{-3}		2·6	4·58	0·17
Tap density/g cm^{-3}		3·166	5·35	0·33
Particle size/μm	D_{10}	4·41	13·36	3·05
	D_{50}	10·24	28·39	7·6
	D_{90}	28·39	57·35	16·8

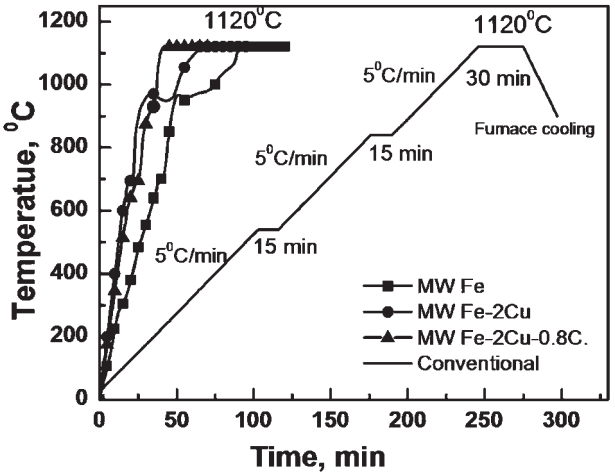

1 Thermal profile followed by conventional $MoSi_2$ heated tubular furnace and microwave (MW) furnace to sinter compacts

The sinterability of the compact was also determined through a densification parameter, which is expressed as

$$\text{Densification parameter} = \frac{\text{Sintered density} - \text{Green density}}{\text{Theoretical density} - \text{Green density}} \tag{2}$$

The sintered samples were polished on a series of SiC emery papers (paper grades 220, 320, 500 and 1000), followed by cloth polishing using a suspension of 0·05 μm alumina diluted with water, and the polished samples were etched with 3% nital to examine the microstructures. The microstructural analysis of the samples was carried out through optical microscope (model DM2500, Leica Imaging System Ltd, Cambridge, UK). The pore size was estimated by measuring the pore area, while the pore shape was characterised using a shape form factor F, which is related to the pore surface area A and its circumference in the plane of analysis P, as follows

$$F = \frac{4\pi A}{P^2} \tag{3}$$

where A is the area of pore (μm^2), and P is the circumference of pore in plane of observation (μm).

Both pore area distribution and shape factor were directly measured using an image analyser. The pore measurement was performed on unetched samples. For each sample, pore shape quantification was performed on 10 photomicrographs captured randomly. Overall, between 3500 and 5700 pores were quantified for statistical accuracy. The shape factor of a feature is inversely proportional to its roundness. A shape factor of 1 represents a circular pore in the plane of analysis, and as it reduces, the pores tend to become more irregular. Bulk hardness of the samples was measured using a semiautomatic Rockwell hardness tester (4150AK, Indentec hardness testing machines Ltd, UK) at 100 kg load with a 16 in. ball indenter. The observed hardness values are the averages of ten readings taken at random spots throughout the sample. The load was applied for 5 s. Tensile testing and transverse rupture strength (TRS) were carried out after each sample marked with 25·4 and 26 mm gauge length using a universal testing machine (1195, Instron, UK) of capacity 20 kN at a strain rate of

$3{\cdot}3 \times 10^{-4}$ s^{-1} (crosshead speed of 0·5 mm min^{-1}). In order to ensure repeatability, for each condition, three samples were evaluated. To correlate the tensile properties with the microstructure, fractography analyses of the samples were carried out using SEM imaging (Zeiss Evo 50, Carl Zeiss SMT Ltd, UK).

Results and discussion

Heating profile

Figure 1 compares the thermal profiles of Fe, Fe–2Cu and Fe–2Cu–0·8C under microwave and conventional heating. All the samples were coupled with microwaves and heated up rapidly. The overall heating rate in the microwave furnace ranges from 12 to 24°C min^{-1}. The same trend was also achieved by a few other researchers for different metallic materials.[21–24] However, in case of conventional heating, the heating rate was limited to 5°C min^{-1}, and it is mainly to avoid thermal shock in the alumina tube. In addition, isothermal holdings at intermittent temperatures were included to homogenise the temperature. Excluding the cooling time, it takes ~4·5 h to perform one complete sintering cycle in conventional sintering. However, in the case of a microwave furnace, the cycle time is reduced by >60% for one cycle. It can be attributed to the lesser heating volume in the microwave furnace; the microwave sintered samples get cooled faster than the conventionally sintered ones. In case of microwave sintering, differences in heating rate were observed in Fe, Fe–2Cu and Fe–2Cu–0·8C compacts as microwave coupling is more a function of composition of the material. Additionally, the microwave sintering profiles show a decrease in heating rate ~900°C in case of Fe and Fe–Cu and are attributed to alpha (α) to gamma (γ) phase transformation. Despite such a fast heating rate, no micro- or macrocracking was observed in all the microwave sintered samples. This underscores the effectiveness of volumetric heating associated with microwaves. Furthermore, for both heating modes, no distortion was observed in the sintered samples.

Densification response

Table 2 compares the densification responses of Fe, Fe–2Cu and Fe–2Cu–0·8C compacts for both conventional and microwave modes of heating. The sintered densities achieved for samples sintered in both routes have no significant difference. It can be clearly seen that compared to theoretical density, the achieved sintered density is lower by ~10%. This is due to the low sintering temperature with short soaking time during sintering. It is interesting to note that even with less processing time in case of microwave sintering, it was possible to achieve similar sinter density due to the faster heating rate, which is responsible for the rapid densification. In order to account for the effect of green density on the sintered density, the densification parameter was quantified in terms of densification parameter. It is a normalised parameter that takes into consideration the initial variation in green density on the densification response. The densification parameters in conventionally sintered samples Fe–2Cu show less densification parameter than others. This confirms the compact swelling due to copper growth phenomenon. The densification parameter is more positive for Fe–2Cu–0·8C than both Fe and Fe–2Cu alloys. This shows the role of carbon in improving the densification response of copper steel by restricting the growth of copper. Comparing both processing routes, the microwave sintered samples show a more positive densification parameter than conventional ones. The enhanced densification in microwave compacts is attributed to the faster heating rate, which restricts the grain coarsening;[25] consequently, grain boundary diffusion is expected to be more pronounced in case of microwave sintering due to the restricted microstructural coarsening.[26,27]

Microstructure evolution

Figure 2 shows optical micrographs of pure Fe, Fe–2Cu and Fe–2Cu–0·8C compacts sintered through conventional and microwave routes. It is clear from the micrographs that for both sintering routes, Fe has the lower porosity with the least pore size. The size of the pore for all the samples was found to be between 0·7 and 0·8 μm. On the other hand, the number of spherical pores in the microwave sintered samples is higher as compared to the conventionally sintered samples. It can be easily visualised in pore shape factor graph in Fig. 3. It has been observed from the micrograph of Fe–2Cu that there are non-homogeneously distributed copper concentrated regions after sintering. This is because at room temperature, the solubility of copper in iron is ~0·4%, which is much less as compared to the initial amount; hence, the excess copper precipitates out, and the regions of higher copper concentrations appear more brownish on the micrograph. Upon comparing the amount of copper precipitate, the microwave sintered samples have less precipitates. This is because microwave prevents grain coarsening due to the fast rate of heating, and also during cooling, it gets cooled at a faster rate, which results in finer precipitates of copper.

Pore evolution

Figure 3 shows the distribution of pore shape factor for all three sintered compositions in both conventional and microwave sintering routes. The dark regions in the microstructure are the pores. The area fractions of each pore were calculated through pixel counting method

Table 2 Effect of heating mode on densification of Fe, Fe–2Cu and Fe–2Cu–0·8C compacts sintered at 1120°C with 30 min soaking time*

	Green density ρ_g/g cm^{-3}		Sintered density ρ_s/g cm^{-3}		Sintered density/% Theor.		Densification parameter	
Composition	C	M	C	M	C	M	C	M
Fe	6·46±0·06	6·32±0·01	6·8±0·4	6·95±0·04	86·5±5·5	88·4±0·56	0·29±0·34	0·41±0·03
Fe–2Cu	6·56±0·13	6·34±0·03	6·9±0·5	6·91±0·02	87·3±6	87·95±0·2	0·24±0·29	0·381±0·02
Fe–2Cu–0·8C	6·49±0·11	6·49±0·01	7·0±0·07	7·14±0·04	91·0±1	92·36±0·46	0·45±0·09	0·54±0·03

*C denotes conventionally sintered, and M denotes microwave sintered.

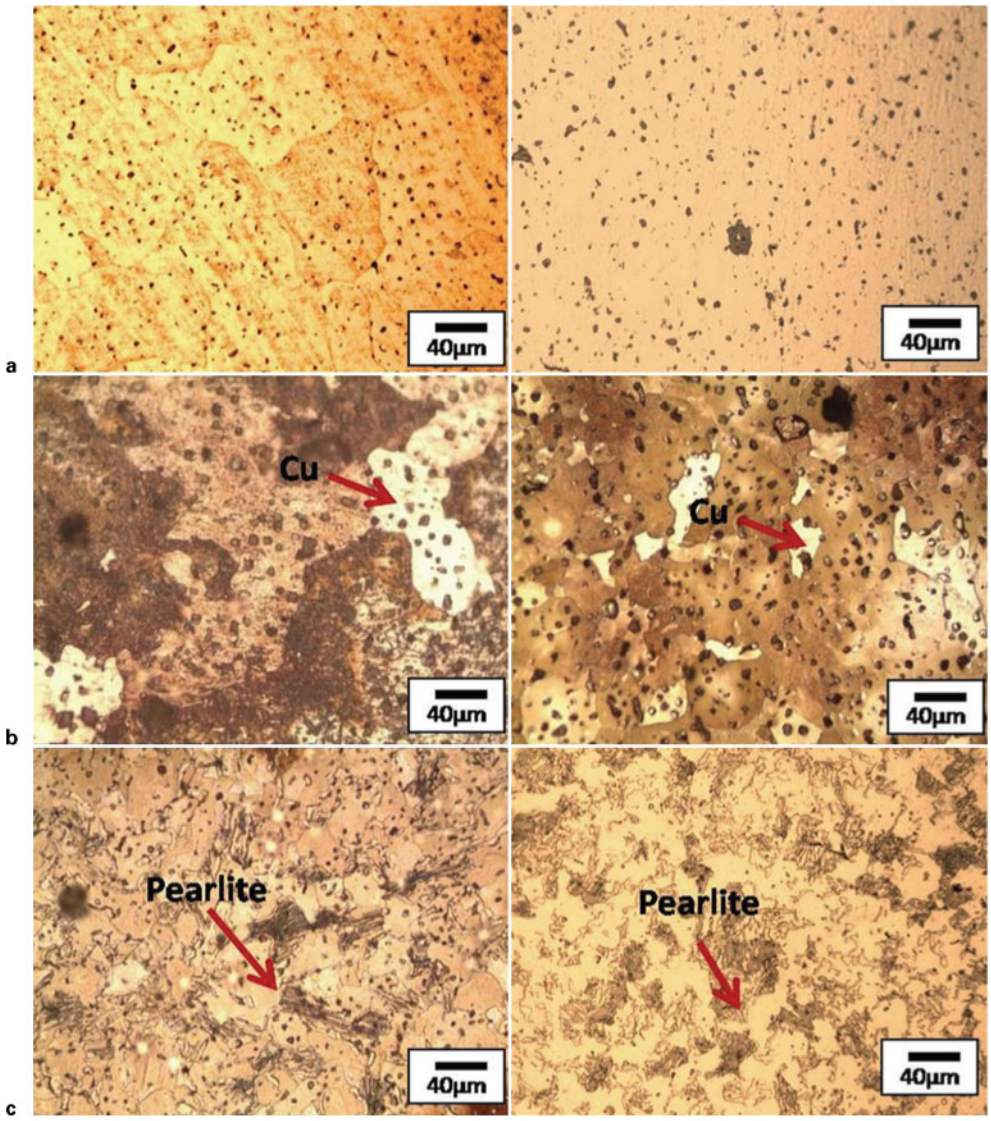

2 Etched optical microstructures of *a* pure Fe, *b* Fe–2Cu and *c* Fe–2Cu–0·8C sintered at 1120°C for 30 min in 90%N_2/10%H_2 atmosphere sintered in conventional (left) and microwave routes (right)

using Image analysing software in a Leica microscope. For homogenous microstructural features, the point fraction, area fraction and volume fraction are equal.[28] The shape factor gives a quantitative measure of pore morphology. A shape factor unity ($F=1$) represents a circular pore in the plane of analysis, and as the number decreases from 1, the degree of irregularity increases. The microwave sintered samples resulted in smaller and narrower pore shape factor distribution, and it slightly skews towards 1, which is an indicative of a more circular pore shape, whereas the conventionally sintered compacts exhibit a broader distribution. This type of improvement in pore shape is also observed by Anklekar *et al.*[12,13] for microwave sintered copper steels.

Mechanical properties

Table 3 shows effect of heating mode on the mechanical properties of Fe, Fe–2Cu and Fe–2Cu–0·8C compacts sintered at 1120°C with 30 min soaking time. Hardness increases with the addition of alloying elements for both routes. The hardness of iron is improved with the addition of copper and carbon for both processing routes. The increase in hardness with the addition of copper is due to solid solution and precipitation hardening, whereas the addition of carbon increases the hardness due to the formation of a pearlite structure. The presence of pearlite was clearly seen in the optical images (Fig. 2). The microwave sintered Fe samples yielded better hardness increment compared to conventional samples. This is due to microwave processing that provides uniform heating and minimises grain coarsening as a result of the fine microstructure with improved hardness observed. In case of microwave sintered Fe–2Cu and Fe–2Cu–0·8C, the samples yielded statistically equivalent hardness when compared to conventional samples. The tensile strength of iron is improved with the addition of copper and carbon for both processing routes. In case of the addition of copper, the increase in tensile strength is attributed to the formation of solid solution and precipitation hardening. While in case of Fe–2Cu–0·8C, the improvement in mechanical properties is due to the formation of a pearlite structure in addition to copper effect, which is clearly seen from optical micrographs (Fig. 2). In general, the microwave

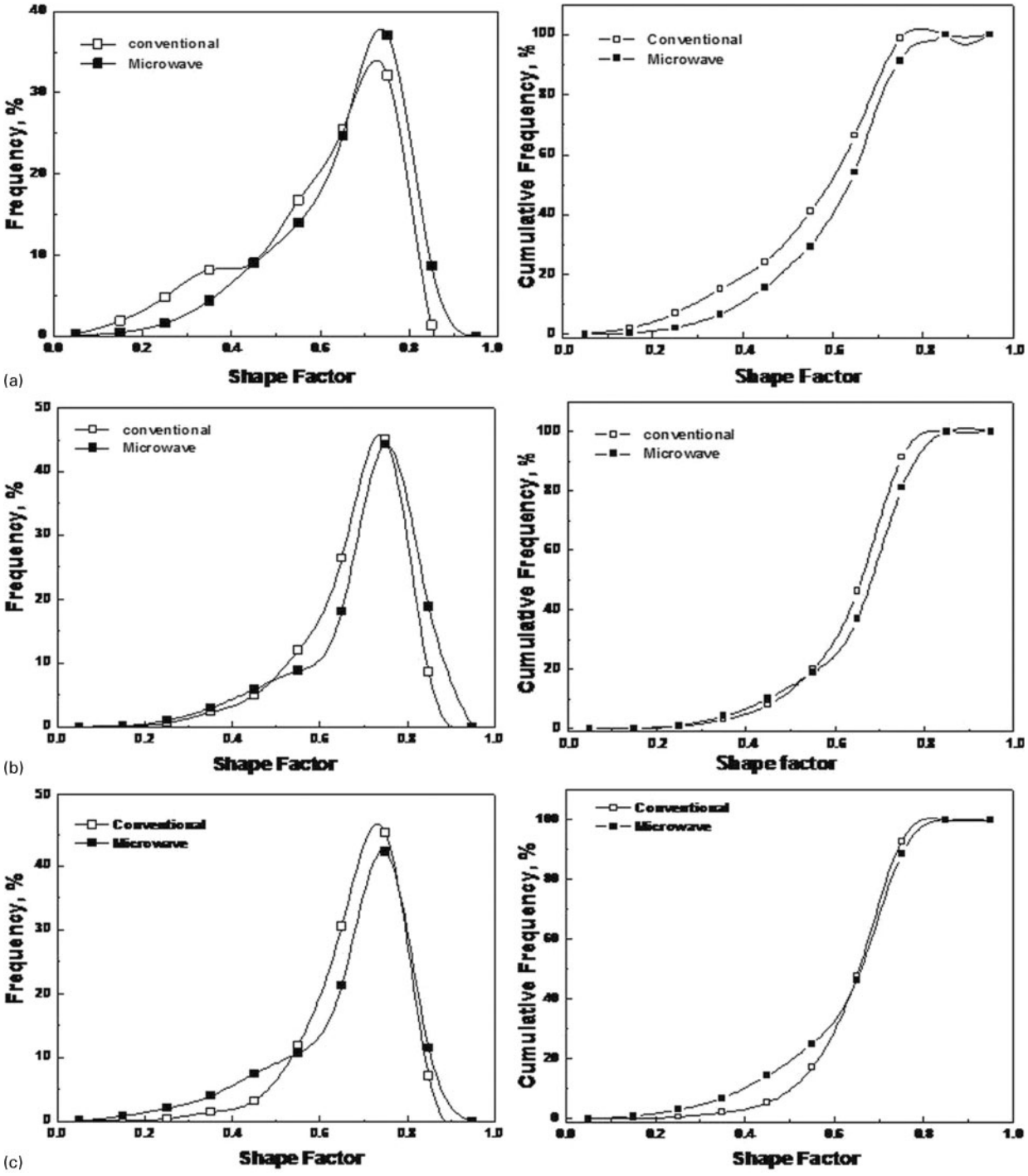

3 Distribution of pore shape form factor for *a* Fe, *b* Fe–2Cu and *c* Fe–2Cu–0·8C: compositions sintered in conventional microwave route

Table 3 Effect of heating mode on mechanical properties of Fe, Fe–2Cu and Fe–2Cu–0·8C compacts sintered at 1120°C with 30 min soaking time*

	Hardness/HRB		Strength/MPa		Elongation/%		TRS	
Composition	C	M	C	M	C	M	C	M
Fe	7±2	18±1·5	126±18	250±6	10±0·12	22±1·24	371±27	501±19
Fe–2Cu	49±7	55±1·8	183±11	389±10	1·6±0·32	19±0·80	638±18	663±30
Fe–2Cu–0·8C	65±3	70±2·5	206±3	408±12	2·6±0·01	9±0·36	841±24	948±21

*C denotes conventionally sintered, and M denotes microwave sintered.

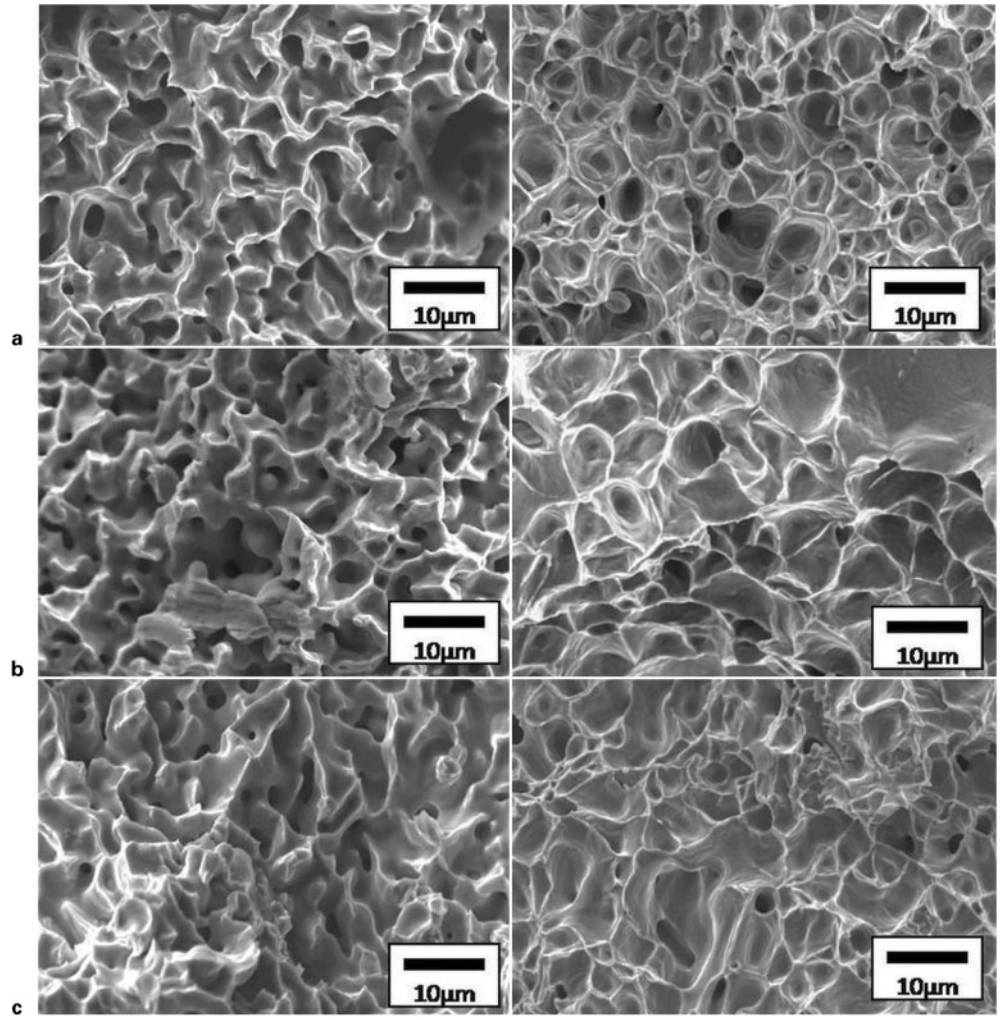

4 Fractographs (SEM) of *a* pure Fe, *b* Fe–2Cu and *c* Fe–2Cu–0·8C tensile test specimen's sintered at 1120°C for 30 min in 90%N_2/10%H_2 atmosphere in conventional (left) and microwave routes (right)

sintered samples showing higher strength than the conventional ones can be attributed to more number of circular pores existing in the compacts.

The ductility of iron is decreased with the addition of copper and carbon for both processing routes. This is because the addition of copper and carbon increased the strength and hardness at the cost of ductility. The microwave sintered samples showed higher ductility than conventional ones. This is also attributed to the nature of pores observed in the microwave processed samples. As it is confirmed from pore shape analysis, the pores in the microwave sintered samples exhibited a more rounded shape than the conventional ones. Hence, crack initiation at pores will be more restricted. From the fractographs of the conventionally sintered parts, more interconnected pores and large cavities are shown. The TRS of the sintered samples increases with the addition of copper and graphite for both sintering routes. The microwave sintered samples have marginal increment compared to their counterparts. The trend observed here is similar to that of ultimate tensile strength. Similar results were observed by Anklekar *et al.*[12,13] They have conducted ductility test for Fe–2Cu–0·8C steel cylindrical tubular samples sintered at 1260°C for a soak time of 20 min using both microwave and conventional sintering.

Figure 4 shows the fractographs of the sintered samples of both routes. It is clear from these micrographs that the conventional sintered samples exhibited microvoid coalescence that has produced shear dimples and lips with characteristic elongated shape. Shear dimples are formed in the presence of large amounts of shear deformation or slip, which is caused by resolved shear stress. The microwave sintered samples show small equiaxed dimples within dimples of moderate sizes and very tiny voids in the membranes (lip or rim) separating the dimples. Here, the dimples are relatively uniform and moderate in size and are very deep, indicating the plastic nature of the material. These types of dimples are created when the failure is caused by normal tensile stress. In case of the amount of cavities created by growth and coalescence of microvoids, the conventionally sintered samples showed large, elongated cavities than the microwave sintered samples. As a result, the microwave samples have better ductility than the conventional samples. This is because the amount of metal to metal contact area is less in conventional samples due to large cavities and hence lesser resistance to support the load.

Conclusions

In the present study, the effects of alloy addition and mode of heating on densification response, microstructural evolution and mechanical property response of Fe, Fe–2Cu and Fe–2Cu–0·8C were investigated. As

compared to conventional furnace heating, the sintering cycle time in a microwave furnace was reduced by ~60%. Despite their reduced processing time, the microwave sintered compacts exhibited higher density and hardness as compared to their conventionally sintered counterparts. This can be attributed to lesser microstructural coarsening during microwave sintering. Pore shape quantification revealed that the microwave sintered samples have more circular porosity as compared to the conventional sintered ones, which helped to improve the mechanical properties of the microwave sintered samples. The conventional sintered samples showed shear dimples and shear lips with characteristic elongated shape, whereas the microwave sintered samples showed small equiaxed dimples, and the dimples were of moderate size, and very tiny voids in the membranes separating the dimples, which lead to stress concentration.

Acknowledgement

The authors would like to acknowledge Indo-US Science and Technology Forum (IUSSTF), New Delhi, for partial support of this research work.

References

1. D. Berner, H. Exner and G. Petzow: *Mod. Dev. Powder Metall.*, 1973, **6**, 237–250.
2. W. Kaysser, W. Huppmann and G. Petzow: *Powder Metall.*, 1980, **23**, 86–91.
3. K. Tabeshfar and G. A. Chadwick: *Powder Metall.*, 1984, **27**, 19–27.
4. S. Banerjee and P. G. Mukunda: *Powder Metall.*, 1984, **27**, 89–92.
5. S. Jamil and G. Chadwick: *Powder Metall.*, 1985, **28**, 65–71.
6. N. Dautzenberg and H. Dorweiler: *Powder Metall. Int.*, 1985, **17**, (6), 279–282.
7. R. Lawcock and T. Davies: *Powder Metall.*, 1990, **33**, 147–150.
8. Y. Wanibe, H. Yokoyama and T. Itoh: *Powder Metall.*, 1990, **33**, (1), 65–69.
9. R. Roy, D. K. Agrawal, J. Cheng and S. Gedevanishvili: *Nature*, 1999, **399**, 668–670.
10. R. Roy, D. Agrawal and J. Cheng: 'Process for sintering powder metal components', US Patent 6,183,689, 2001.
11. R. M. Anklekar, K. Bauer, D. K. Agrawal and R. Roy: Proc. 2nd National Powder Metallurgy Conf., (ed. S. Sarita), 287–95; 1999, Ankara Turkey, Middle East Technical University.
12. R. M. Anklekar, D. K. Agrawal and R. Roy: *Powder Metall.*, 2001, **44**, (4), 355–362.
13. M. Anklekar, K. Bauer, D. K. Agrawal and R. Roy: *Powder Metall.*, 2005, **48**, (1), 39.
14. 'MPIF standard 48: determination of apparent density of metal powders using the Arnold meter', 'Standard test methods for metal powders and powder metallurgy products', Metal Powder Industries Federation, Princeton, NJ, USA, 1991.
15. 'MPIF standard 46: determination of tap density of metal powder', 'Standard test methods for metal powders and powder metallurgy products', Metal Powder Industries Federation, Princeton, NJ, USA, 1991.
16. 'MPIF standard 3: determination of flow rate of free flowing metal powders using the hall apparatus', 'Standard test methods for metal powders and powder metallurgy products', Metal Powder Industries Federation, Princeton, NJ, USA, 1991.
17. E. Pert, Y. Carmel, A. Birnboim, T. Olorunyolemi, D. Gershon, J. Calame, I. Lloyd and O. Wilson: *J. Am. Ceram. Soc.*, 2001, **84**, 1981.
18. D. R. Lide (ed.): 'CRC handbook of chemistry and physics', 79th edn; 1998, Boca Raton, FL, CRC Press.
19. A. Nayer (ed.): 'The metals data book'; 1997, New York, NY, McGraw-Hill.
20. M. Mizuno, S. Obata, S. Takayama, S. Ito, N. Kato, T. Hirai and M. Sato: 'Sintering of alumina by 2·45 GHz microwave heating', *J. Eur. Ceram. Soc.*, 2004, **24**, 387–391.
21. Kuen-Shyang Hwang, Yung-Chung Lu, Guo-Jiun Shu and Bor-Yuan Chen: *Metall. Mater. Trans. A*, 2009, **40A**, 3217.
22. A. Mondal, A. Upadhyaya and D. Agrawal: *Mater. Sci. Eng. A*, 2010, **A527**, 6870–6878.
23. A. Upadhyaya, S. K. Tiwari and P. Mishra: *Scr. Mater.*, 2007, **56**, 5–8.
24. K. Saitou: *Scr. Mater.*, 2006, **54**, (5), 875–879.
25. S. J. Kang: 'Sintering: densification, grain growth and microstructure'; 2005, London, Elseiver Butterworth-Heinemann.
26. S. S. Sahay and K. Krishnan: *Physica B*, 2004, **348B**, 310–314.
27. S. S. Sahay and K. Krishnan: *Thermochim. Acta*, 2005, **430**, 23–39.
28. E. E. Underwood: 'Quantitative stereology'; 1981, Reading, MA, Addison-Wesley Pub. Co.